

# Multicolor Operation and Spectral Control in a Gain-Modulated X-ray Free Electron Laser \*

A. Marinelli<sup>1</sup>, A.A. Lutman<sup>1</sup>, J. Wu<sup>1</sup>, Y. Ding<sup>1</sup>, J. Krzywinski<sup>1</sup>, H. D. Nuhn<sup>1</sup>, Y. Feng<sup>1</sup>, R. Coffee<sup>1</sup>, C. Pellegrini<sup>2</sup>

<sup>1</sup> SLAC National Accelerator Laboratory, Menlo Park, CA 94025, USA

<sup>2</sup> Department of Physics and Astronomy, University of California Los Angeles, Los Angeles, CA 90095, USA

## Abstract

We show that modulating the gain in magnetic undulators can control the spectral properties of a SASE x-ray free-electron laser, producing one or several spectral lines within a single few femtosecond pulse. By varying the magnetic field along the undulator and the electron beam transport line, the system we propose can tailor the X-ray spectrum to optimally meet numerous experimental requirements such as spectral narrowing, broadening, or multi-color operation.

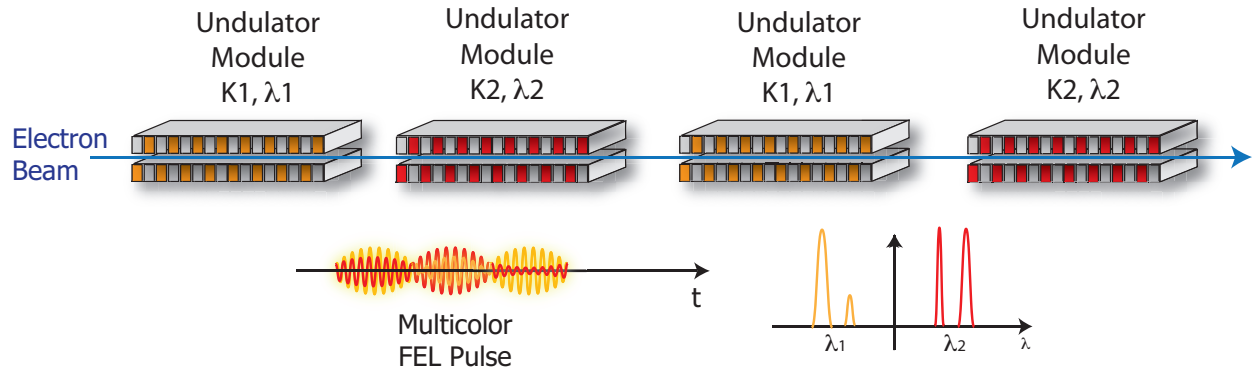


Figure 1: Schematics of a gain-modulated FEL.

The x-ray free-electron laser (xFEL) is the brightest source of coherent radiation in the nanometer and subnanometer wavelength regime. Operational xFEL facilities such as LCLS [1], SACLA [2] and FLASH [3] have already shown remarkable scientific capabilities in biology, chemistry, material science, atomic and molecular physics as well as many other disciplines (see e.g. Refs. [4, 5, 6]). These existing xFEL facilities operate in the self-amplified spontaneous emission (SASE) mode, and as a result, their spectrum is extremely noisy with a bandwidth of the order of the FEL parameter  $\rho$  [7], typically about 0.001. Such pulse may be nearly diffraction limited but they are certainly not Fourier limited given typical temporal profiles composed of several uncorrelated spectral spikes [8]. Several methods have been proposed to improve the FEL temporal (longitudinal) coherence using external laser seeding [9, 10, 11] or self-seeding [12, 13]. More recently, however, it has been shown that near Fourier limited pulses can be obtained by delaying the electron bunch with respect to the radiation pulse in a controlled way, a technique known as iSASE [14] which follows ideas originally developed in the context of mode-locked FELs [15].

Two-color operation of x-ray FELs has recently been the subject of intense research at x-ray user facilities because of its high desirability for coherent diffraction bio-imaging, condensed matter x-ray spectroscopy, and even multiphoton x-ray processes in atomic and molecular systems. First observed with an infrared FEL oscillator [16], two-color operation of a high-gain x-ray free-electron laser has been recently demonstrated in the soft x-ray regime in Ref. [17] and also for a seeded FEL in Ref. [18]. In contrast to Ref. [17], however, the so called gain-modulated FEL reported here can achieve two-color pulses within one slippage length, allowing for near simultaneous emission within a time delay much less than the few femtosecond pulse duration. We therefore report the generation of single xFEL pulses comprized of two narrow spectral lines whose photon energy separation can be tuned by as much as 2% of the average photon energy.

The gain-modulated FEL technique shown in Fig. 1 uses periodic modulation of the undulator field to produce either a single narrow x-ray spectral line or multiple lines with controlled, tunable photon energy separation. As we will see below, this technique is analo-

---

\*Work supported by Department of Energy contract DE-AC02-76SF00515.

gous to gain-modulation in solid state lasers. In the case of an FEL, the modulation of the magnetic field of an undulator in an FEL was first explored theoretically for a simple bi-harmonic undulator [19]. In this Letter we show that a periodic modulation of the undulator field is equivalent to introducing a sequence of delays for two different resonant wavelengths. As the electron bunch propagates, the sequence of resonance-delay sections develops an interference pattern that gives rise to multiple spectral lines. Each line has a narrower bandwidth than pure SASE radiation but multiple lines can be distributed over a spectral range that is wider than the intrinsic SASE bandwidth. We present a universally scaled one-dimensional theory of this new mode of operation and present its first experimental demonstration at the Linac Coherent Light Source (LCLS).

A free-electron laser operating in the self-amplified spontaneous emission (SASE) mode, amplifies the beam shot-noise derived microbunching and generates coherent radiation at a central wavelength of:

$$\lambda_r = \lambda_u \frac{1 + \frac{K^2}{2}}{2\gamma^2}, \quad (1)$$

where  $\lambda_u$  is the undulator period,  $\gamma$  is the beam energy normalized to the rest energy  $mc^2$ , and the undulator parameter  $K$  is related to the peak magnetic field of the undulator by:  $K = \frac{eB_u\lambda_u}{2\pi mc^2}$ . The gain bandwidth is of the order of the FEL parameter  $\rho = \left(\frac{K}{4} \frac{\lambda_w \omega_p}{2c\pi}\right)^{1/3}$  [7], where  $c$  is the speed of light and  $\omega_p = \frac{4\pi e^2 n_0}{m\gamma^3}$  is the relativistic beam plasma frequency, with  $n_0$  being the beam volume density and  $m$  the electron mass. The FEL parameter also defines the energy transfer at saturation from the electron beam to the photon pulse. In the SASE mode, the spectrum is composed of several uncorrelated spikes distributed within the amplification bandwidth and the temporal profile is given by several spikes with a characteristic length of  $\lambda_r/\rho$ . In a typical SASE FEL, the undulator parameter  $K$  is constant during the amplification process, except for a small linear taper (on the order of 1% over the entire undulator beamline) that is used to compensate beam energy losses due to spontaneous radiation and wakefields.

The gain-modulated FEL, as shown in Fig. 1, is analogous to gain-modulation in solid state lasers e. g. quantum cascade lasers [20] where a periodic modulation of the active medium gives rise to discrete energy bands that are determined entirely by the geometry of the medium. In the context of FELs, gain modulation is achieved by a series of undulator sections with alternating peak magnetic fields, with periodicity  $L_u$ . This allows for nearly simultaneous generation of two colors in a single pulse, as required by the class of experiments mentioned above. By producing two distinct values of the undulator parameter  $K_{1,2}$ , two resonant wavelengths  $\lambda_{1,2} = \lambda_w \frac{1+K_{1,2}^2}{2\gamma^2}$  are alternately amplified as the beam travels along the undulator. This undulator configuration allows both colors to be simultaneously amplified, allowing for a time separation smaller than the slippage in a single modulation period  $\lambda_r L_u / \lambda_w$ . We note that the separation of the two resonant wavelengths can be even larger than the gain width, if  $2\frac{\lambda_1 - \lambda_2}{\lambda_1 + \lambda_2} \gg \rho$ . This type of configuration can be easily implemented in all existing x-FEL facilities, since typical X-FEL undulators are divided into many sections, and each section has a tunable strength parameter  $K$ .

The evolution of the system in an undulator section can be described with a simple one-

dimensional model. We use the formalism introduced in [8], in which the FEL dynamics is described in terms of three universally scaled collective variables. The radiation electric field  $E_{\text{rad.}}$  is normalized to the saturation power as  $A = E_{\text{rad.}}/(4\pi\rho P_b)^{1/2}$ , where  $P_b = \gamma n_0 m c^2$  is the electron beam power density. The electron beam bunching factor is given by  $B = \frac{1}{N_\lambda} \sum_j e^{-i(k_u + k_{r-1,2})z_j - ikct}$  with the sum performed over the  $N_\lambda$  electrons contained in a region of length  $\lambda_{1,2}$  and  $k_{r-1,2} = 2\pi/\lambda_{1,2}$  is the resonant wavenumber and  $k_u = 2\pi/\lambda_u$ . The energy modulation is then given by  $P = \sum_j \frac{\eta_j}{\rho} e^{-i(k_u + k_{r-1,2})z_j - ikct}$  which is normalized to  $\rho$  where  $\eta_j$  is the relative energy deviation of the  $j$ -th particle. Assuming the linear growth regime, the FEL evolves according to the following [8]

$$\begin{aligned}\frac{\partial A}{\partial \tau} + \frac{\partial A}{\partial \zeta} &= B \\ \frac{\partial B}{\partial \tau} &= P \\ \frac{\partial P}{\partial \tau} &= iA\end{aligned}\tag{2}$$

where the interaction time is normalized to the FEL gain-length as  $\tau = ct/L_g$  with  $L_g = \lambda_u/4\pi\rho$ . The scaled position along the electron bunch is  $\zeta = c(z/v_z - t)/L_c$  where  $v_z$  is the electron velocity along the  $z$ -axis and  $L_c = L_g\lambda_r/\lambda_u$  is the cooperation length. We consider only the case of zero initial energy spread and a bunch length much larger than the cooperation length. Introducing the Fourier transform with respect to the bunch variable we have:

$$\begin{aligned}\frac{\partial A}{\partial \tau} + i\delta A &= B \\ \frac{\partial B}{\partial \tau} &= P \\ \frac{\partial P}{\partial \tau} &= iA\end{aligned}\tag{3}$$

where  $\delta = (\lambda_r - \lambda)/2\lambda_r\rho$  is the normalized detuning and  $\lambda_r$  is the resonant wavelength in each module. In a gain-modulated FEL, for a given wavelength  $\lambda$ ,  $\delta$  has a different value in each undulator module.

The solution of the linear system 3 can be expressed in compact form in terms of a transfer matrix:

$$\begin{pmatrix} B \\ P \\ A \end{pmatrix} = M_\tau(\delta) \begin{pmatrix} B_0 \\ P_0 \\ A_0 \end{pmatrix},\tag{4}$$

where

$$M_\tau(\delta) = I + \sum_{j=1}^3 \frac{i(\exp(i\mu_j\tau) - 1)}{3\mu_j^2 - 2\delta\mu_j} \begin{pmatrix} \frac{i}{\mu_j} & \frac{1}{\mu_j^2} & -i \\ -1 & \frac{i}{\mu_j} & \mu_j \\ i\mu_j & 1 & -i\mu_j^2 \end{pmatrix}.\tag{5}$$

The eigenvalues  $\mu_j$  are the solution of the cubic dispersion equation:

$$\mu^3 - \delta\mu^2 + 1 = 0.\tag{6}$$

Equations 4 and 5 represent the evolution of the beam collective variables in the linear regime through one undulator module.

In a gain-modulated FEL, the undulator is composed of a series of sections with alternating magnetic field which allows for two resonant wavelengths  $\lambda_{1,2}$ . We define the average resonant wavelength as  $\bar{\lambda}_r = (\lambda_1 + \lambda_2)/2$ . For a given wavelength we define an average detuning parameter  $\bar{\delta} = (\bar{\lambda}_r - \lambda)/2\bar{\lambda}_r\rho$  and the normalized frequency separation  $\Delta = (\lambda_2 - \lambda_1)/2\bar{\lambda}_r\rho$ . The FEL dynamics is then described by the following evolution matrix:

$$\begin{pmatrix} B \\ P \\ A \end{pmatrix} = \prod_{n=1}^{N_u} M_{\tau_u}(\bar{\delta} + (-1)^n \Delta) \begin{pmatrix} B_0 \\ P_0 \\ A_0 \end{pmatrix}, \quad (7)$$

where  $\tau_u$  is the normalized length of an undulator section,  $N_u$  is the total number of sections and  $B_0, P_0, A_0$  are the initial values of the collective variables and the normalized radiation field. For small values of the effective detuning  $\delta = \bar{\delta} + (-1)^n \Delta$ , the undulator is resonant and the FEL is in the exponentially growing regime. For large values of the detuning parameter, instead, the single undulator transfer matrix can be approximated as:

$$M \simeq \begin{pmatrix} 1 & \tau_u & 0 \\ 0 & 1 & 0 \\ 0 & 0 & e^{-i\delta\tau_u} \end{pmatrix}. \quad (8)$$

Equation (8) describes the evolution of the system in a non-resonant interaction regime. The microbunching grows linearly as a function of time,  $B = B_0 + P_0\tau_u$ , since the finite undulator dispersion transforms the electron beam energy modulation  $P_0$  into density modulation. The electron bunch slips behind the radiation field to produce a delay term  $e^{-i\delta\tau_u}$ . For large detuning, the induced slippage in the detuned undulator increases the effective cooperation length [14, 15] and thus reducing the spectral bandwidth of each color. Incidentally, this very same physical principle is employed in an improved SASE (iSASE) FEL [14] whereby the delay is induced by magnetic chicanes placed between undulator sections such that the bandwidth can be reduced to very near Fourier limit. Therefore, a gain modulated FEL can be described as a two-color iSASE scheme where each resonant wavelength  $\lambda_{1,2}$  alternates between an exponential growing section and a delay section.

We define the gain function  $G_f$  as the amplitude of the field variable divided by the initial bunching factor  $G_f = |A|/|B_0|$  starting from the following condition  $P_0 = 0, A_0 = 0$ . The gain function is the average spectral power gain in a gain-modulated FEL starting from shot-noise. Figure 2 shows the amplitude squared of the gain function as a function of the detuning parameter  $\bar{\delta}$  and the normalized wavelength separation  $\Delta$  for  $\tau_u = 1/\sqrt{3}$ , corresponding to an undulator periodicity of two power gain-lengths. The spectral power gain is also shown for three different values of  $\Delta$ . The spectral power gain exhibits several peaks, corresponding to the condition  $\bar{\delta}\tau_u = N\pi$ , where  $N$  is an integer number. In physical units, the relative wavelength separation of these peaks corresponds to the periodicity of the undulator modulation divided by the undulator frequency, i.e.  $d\lambda/\lambda = \lambda_w/2L_u$ . At the average detuning value corresponding to the spectral peaks, the average phase advance in every undulator modulation period is exactly  $2\delta_{pk}\tau_u = 2N\pi$ , corresponding to a constructive

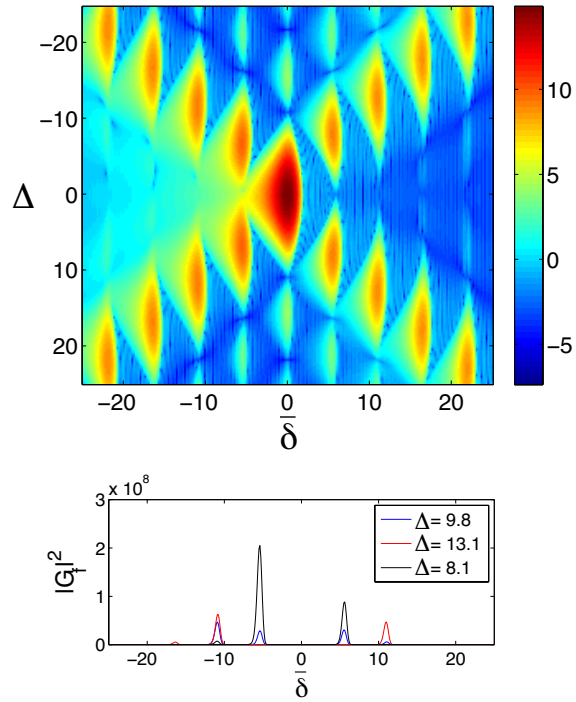


Figure 2: Gain curve (logarithm of the gain function  $G_f$ ) as a function of the average detuning  $\bar{\delta}$  and the undulator detuning  $\Delta$  (upper image). The lower image shows a linear plot of the gain function for three different values of  $\Delta$ .

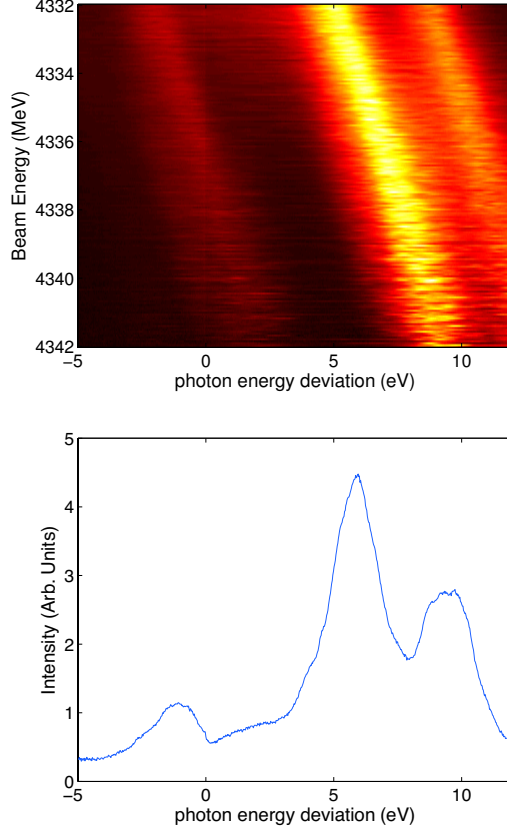


Figure 3: Average intensity as a function of beam energy and photon energy for an undulator periodicity of 2 undulator sections (upper plot). The lower plot shows the average intensity as a function of photon energy for a beam energy of 4336 MeV.

interference between the radiation emitted in two consecutive resonant undulators. The way the power density is distributed among the spectral peaks depends on the relative position of the peaks with respect to the undulator detuning  $\Delta$ . While the exact power density distribution has a rather strong dependence on  $\tau_u$  and  $\Delta$ , the structure of the spectrum roughly follows the following trend: the configurations corresponding to  $\Delta\tau_u \simeq N\pi$  favor the generation of two strong spectral peaks around  $\delta \simeq \pm\Delta$ , while for  $\Delta\tau_u \simeq (N + 1/2)\pi$  the spectral power density is distributed over 4 peaks. Intermediate values of the undulator detuning show a variety of spectral structures with two, three or four dominant peaks. Since the FEL detuning curve is asymmetric, the radiation power is not evenly distributed along the resonant peaks, even in cases where four colors are emitted.

The generation of multicolor pulses with a gain-modulated FEL has been demonstrated experimentally at LCLS. The experimental beam parameters are: energy  $E_b = 4.77\text{GeV}$ , peak current  $I_p = 2\text{kA}$ , normalized transverse emittance  $\epsilon_{x,y} \simeq 0.34\mu\text{m}$ . The average photon energy was tuned to  $E_{ph} \simeq 838\text{eV}$ , corresponding to a wavelength of  $\bar{\lambda}_r = 1.5\text{nm}$ . The pulse duration is limited to  $20\text{fsec}$  full width at half maximum (FWHM) by use of an emittance

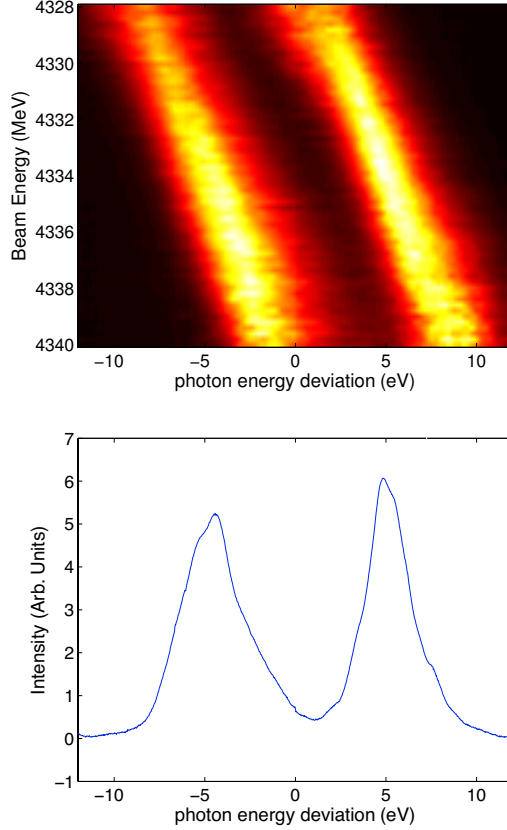


Figure 4: Average intensity as a function of beam energy and photon energy for an undulator periodicity of 6 undulator sections (upper plot). The lower plot shows the intensity as a function of photon energy for a beam energy of 4334 MeV.

spoiler [21]. The spectrum is measured with a soft-x-ray grating spectrometer [22] The LCLS undulator is composed of sections of 110 periods each, which limits the undulator modulation periodicity to multiples of  $220 \lambda_u$  undulator periods. Figure 3 shows the average spectrum as a function of beam energy for a configuration with undulator periodicity of two undulator sections (i.e., alternating the  $K$  value at every undulator section), corresponding to a sideband separation of  $\delta\lambda/\lambda \simeq 0.44\%$ . The data has been binned in energy to deconvolve the effect of shot-to-shot beam energy fluctuations. The spectrum clearly shows the appearance of three lines, spaced by multiples of the normalized undulator periodicity. The measured pulse energy  $E_{pl} \simeq 15\mu J$  is roughly one tenth of the SASE pulse energy for the same beam conditions.

By increasing the periodicity of the undulator modulation, the spectral separation of the emission peaks decreases. Figure 4 shows the spectral intensity as a function of photon energy and beam energy for a configuration with a modulation periodicity of six undulators. In this case, the sidebands merge into one dominant peak and the two emitted colors correspond to the resonant wavelengths in the alternating undulators. Note that the saturation length of



the FEL is not normally a multiple of the modulation period, which means that typically one color contains a larger number of photons. For certain scientific applications, however, it is important that the two colors have the same intensity. This problem can be easily overcome by adding a few extra undulators to boost the emitted photons in one of the two colors. Balancing of the two colors is achieved in this case by adding five undulators tuned to the low-energy photon pulse close to the saturation point. The pulse energy in this case was roughly  $E_p = 18\mu J$ , with a pulse duration of  $10\text{fsec}$  determined by the emittance spoiler aperture.

In conclusion, in this Letter we introduce the concept of gain-modulated FELs. In this new mode of operation, the magnetic field of the undulator is modulated periodically by alternating the undulator parameter  $K$  with a certain periodicity. The spectrum of a gain-modulated FEL is composed of several lines. Each line has a bandwidth smaller than that of SASE but their separation can be larger than the SASE bandwidth itself. We discuss a simple universally scaled model of this process and present the first experimental demonstration at the LCLS. The results presented in this Letter extend the capabilities of x-ray free-electron lasers by allowing the generation of a single x-ray pulse with multiple spectral lines with tunable photon energy separation.

The authors would like to acknowledge Z. Huang and M. E. Couprie for useful discussions and suggestions.

## References

- [1] P Emma et al. First lasing and operation of an angstrom-wavelength free-electron laser. *Nat Photon*, 4:641–647, Aug 2010.
- [2] T. Ishikawa, H. Aoyagi, T. Asaka, and al. A compact x-ray free-electron laser emitting in the sub-angstrom region. *Nat Photon*, 6:540–544, Aug 2012.
- [3] W Ackermann, G Asova, V Ayvazyan, A Azima, N Baboi, J Bähr, V Balandin, B Beutner, A Brandt, A Bolzmann, et al. Operation of a free-electron laser from the extreme ultraviolet to the water window. *Nature photonics*, 1(6):336–342, 2007.
- [4] N. Rohringer, D. Ryan, R. London, M. Purvis, and al. Atomic inner-shell x-ray laser at 1.46 nanometres pumped by an x-ray free-electron laser. *Nature*, 481:488–491, 2012.
- [5] H. N. Chapman, P. Fromme, A. Barty, T. A. White, R. A. Kirian, and al. Femtosecond x-ray protein nanocrystallography. *Nature*, 470:73–77, 2011.
- [6] M. M. Seibert, Ekeberg T., F. Maia, M. Svenda, and al. Single mimivirus particles intercepted and imaged with an x-ray laser. *Nature*, 470:78–81, 2011.
- [7] R. Bonifacio, C. Pellegrini, and L.M. Narducci. Collective instabilities and high-gain regime in a free-electron laser. *Optics Communications*, 50(6):373–378, Jul 1984.

- [8] R. Bonifacio, L. De Salvo, P. Pierini, N. Piovella, and C. Pellegrini. Spectrum, temporal structure, and fluctuations in a high-gain free-electron laser starting from noise. *Phys. Rev. Lett.*, 73(1):70–73, Jul 1994.
- [9] G Lambert, T Hara, D Garzella, T Tanikawa, M Labat, B Carre, H Kitamura, T Shintake, M Bougeard, S Inoue, et al. Injection of harmonics generated in gas in a free-electron laser providing intense and coherent extreme-ultraviolet light. *Nature Physics*, 4(4):296–300, 2008.
- [10] L.-H. Yu, M. Babzien, I. Ben-Zvi, L. F. DiMauro, A. Doyuran, W. Graves, E. Johnson, S. Krinsky, R. Malone, I. Pogorelsky, J. Skaritka, G. Rakowsky, L. Solomon, X. J. Wang, M. Woodle, V. Yakimenko, S. G. Biedron, J. N. Galayda, E. Gluskin, J. Jagger, V. Sajaev, and I. Vasserman. High-gain harmonic-generation free-electron laser. *Science*, 289(5481):932–934, 2000.
- [11] E Allaria, R Appio, L Badano, WA Barletta, S Bassanese, SG Biedron, A Borga, E Busetto, D Castronovo, P Cinquegrana, et al. Highly coherent and stable pulses from the fermi seeded free-electron laser in the extreme ultraviolet. *Nature Photonics*, 2012.
- [12] J. Feldhaus, E. L. Saldin, J. R. Schneider, E. A. Schneidmiller, and M. V. Yurkov. Possible application of x-ray optical elements for reducing the spectral bandwidth of an x-ray sase fel. *Optics Communications*, 140(4-6):341 – 352, 1997.
- [13] J Amann, W Berg, V Blank, F-J Decker, Y Ding, P Emma, Y Feng, J Frisch, D Fritz, J Hastings, et al. Demonstration of self-seeding in a hard-x-ray free-electron laser. *Nature Photonics*, 2012.
- [14] J. Wu, A. Marinelli, and C. Pellegrini. X-ray free electron lasers spectrum control with improved self-amplified spontaneous emission. *Submitted to Nat. Photonics*, 2013.
- [15] N. R. Thompson and B. W. J. McNeil. Mode locking in a free-electron laser amplifier. *Phys. Rev. Lett.*, 100:203901, May 2008.
- [16] D. A. Jaroszynski, R. Prazeres, F. Glotin, and J. M. Ortega. Two-color free-electron laser operation. *Phys. Rev. Lett.*, 72:2387–2390, Apr 1994.
- [17] A. A. Lutman, R. Coffee, Y. Ding, Z. Huang, J. Krzywinski, T. Maxwell, M. Messerschmidt, and H.-D. Nuhn. Experimental demonstration of femtosecond two-color x-ray free-electron lasers. *Phys. Rev. Lett.*, 110:134801, Mar 2013.
- [18] Giovanni De Ninno, Beno<sup>^</sup>Mahieu, Enrico Allaria, Luca Giannessi, and Simone Spampinati. Chirped seeded free-electron lasers: Self-standing light sources for two-color pump-probe experiments. *Phys. Rev. Lett.*, 110:064801, Feb 2013.
- [19] G. Dattoli, V. V. Mikhailin, P. L. Ottaviani, and K. V. Zhukovsky. Two-frequency undulator and harmonic generation by an ultrarelativistic electron. *Journal of Applied Physics*, 100(8):084507, 2006.

- [20] Jerome Faist, Federico Capasso, Deborah L. Sivco, Carlo Sirtori, Albert L. Hutchinson, and Alfred Y. Cho. Quantum cascade laser. *Science*, 264(5158):553–556, 1994.
- [21] P. Emma, K. Bane, M. Cornacchia, Z. Huang, H. Schlarb, G. Stupakov, and D. Walz. Femtosecond and subfemtosecond x-ray pulses from a self-amplified spontaneous-emission-based free-electron laser. *Phys. Rev. Lett.*, 92:074801, Feb 2004.
- [22] Philip Heimann, Oleg Krupin, William F. Schlotter, Joshua Turner, Jacek Krzywinski, Florian Sorgenfrei, Marc Messerschmidt, David Bernstein, Jaromir Chalupsky, Vera Hajkova, Stefan Hau-Riege, Michael Holmes, Libor Juha, Nicholas Kelez, Jan Luning, Dennis Nordlund, Monica Fernandez Perea, Andreas Scherz, Regina Soufli, Wilfried Wurth, and Michael Rowen. Linac coherent light source soft x-ray materials science instrument optical design and monochromator commissioning. *Review of Scientific Instruments*, 82(9):093104, 2011.